Published in final edited form as:

Matrix Biol. 2018 April ; 67: 90–106. doi:10.1016/j.matbio.2017.12.003.

Extracellular Matrix Directs Phenotypic Heterogeneity of Activated Fibroblasts

Diana Avery[a,b], **Priya Govindaraju**[a,b], **Michele Jacob**[c], **Leslie Todd**[a], **James Monslow**[a], and **Ellen Puré**[a,b]

[a]Department of Biomedical Sciences, University of Pennsylvania, Philadelphia, PA

[b]Pharmacology Graduate Group of the University of Pennsylvania, Philadelphia, PA

Abstract

Activated fibroblasts are key players in the injury response, tumorigenesis, fibrosis, and inflammation. Dichotomous outcomes in response to varied stroma-targeted therapies in cancer emphasize the need to disentangle the roles of heterogeneous fibroblast subsets in physiological and pathophysiological settings. In wound healing, fibrosis, and myriad tumor types, fibroblast activation protein (FAP) and alpha-smooth muscle actin (αSMA) identify distinct, yet overlapping, activated fibroblast subsets. Prior studies established that FAP^{Hi} reactive fibroblasts and $αSMA^{Hi}$ myofibroblasts can exert opposing influences in tumorigenesis. However, the factors that drive this phenotypic heterogeneity and the unique functional roles of these subsets have not been defined. We demonstrate that a convergence of ECM composition, elasticity, and transforming growth factor beta (TGF-β) signaling governs activated fibroblast phenotypic heterogeneity. Furthermore, FAP^{Hi} reactive fibroblasts and $αSMA^{Hi}$ myofibroblasts exhibited distinct gene expression signatures and functionality *in vitro*, illuminating potentially unique roles of activated fibroblast subsets in tissue remodeling. These insights into activated fibroblast heterogeneity will inform the rational design of stroma-targeted therapies for cancer and fibrosis.

Keywords

Activated fibroblasts; Fibroblast activation protein; Alpha-smooth muscle actin; Fibroblast heterogeneity

1.1 Introduction

In development and homeostasis, fibroblasts synthesize extracellular matrix (ECM), which regulates cell differentiation and behavior. As sentinel cells, fibroblasts respond to injury and neoplasia by differentiating to highly secretory, proliferative, or contractile phenotypes. This

Corresponding Author: Ellen Puré, epure@upenn.edu, University of Pennsylvania School of Veterinary Medicine, Old Vet Quad, Office 216E, 3800 Spruce Street, Philadelphia, PA 19104.
[c]Current affiliation: Envision Pharma Group, Philadelphia, PA

heterogeneous activated fibroblast population orchestrates injury resolution. However, in fibrosis and cancer, the aberrant accumulation of activated fibroblasts and ECM disrupts organ function [1–5].

Fibroblast activation protein (FAP) is a marker of activated fibroblasts in the injury response[6], fibrotic and inflammatory conditions [7–9], and myriad tumor types [10–14]. In most epithelial-derived tumors, FAP and alpha smooth muscle actin (αSMA; the canonical myofibroblast marker) identify distinct, yet overlapping, fibroblast subsets [11,12,15–17]. Importantly, FAP^{Hi} fibroblasts and αSMA^{Hi} myofibroblasts diverge in their impact on tumorigenesis. FAP^{Hi} fibroblasts accelerate the growth of multiple tumor types by promoting intratumoral desmoplasia, angiogenesis, and immunosuppression [11,18–20]. In contrast, αSMA^{Hi} myofibroblasts reportedly can curb pancreatic cancer aggressiveness by restraining epithelial-mesenchymal transition, cancer stem cell generation, and immunosuppression [15]. FAP and αSMA similarly mark distinct fibroblast subsets in fibrotic conditions, including idiopathic pulmonary fibrosis and liver cirrhosis [7,8]. However, the conditions regulating this phenotypic heterogeneity and the unique functional roles of these phenotypically distinct subsets are not yet known. Disentangling these complexities will clarify the roles of heterogeneous fibroblast subsets in physiological and pathophysiological settings.

ECM composition and mechanics exhibit spatiotemporal heterogeneity in acute injury, fibrosis, and cancer [21–26]. Notably, both granulation tissue and intratumoral desmoplasia evolve from elastic, fibronectin (FN)-rich to stiff, collagen I (COL 1)-rich ECM [25,27–30]. Therefore, we hypothesized that ECM properties directly regulate fibroblast heterogeneity. To test this hypothesis, we assessed fibroblast activation on substrata of defined stiffness and composition. Gene expression analysis revealed distinct signatures, illuminating potentially unique functional roles of FAP^{Hi} fibroblasts and αSMA^{Hi} myofibroblasts in tissue remodeling, consistent with the distinct functionalities we observed *in vitro*. These insights will help foster the rational design and clinical application of stromal cell-targeted therapies in cancer and fibrosis.

1.2 Results

1.2.1 Substratum directs activated fibroblast phenotypic heterogeneity

Primary murine adult pulmonary fibroblasts were cultured on tissue culture-treated plastic for 2 passages, which generated a heterogeneous population of activated fibroblasts with variable levels of FAP and αSMA (data not shown). These fibroblasts were reseeded on plastic and the impact of soluble mediators thought to promote fibroblast activation [31–33] on *Fap* and *Acta2* (αSMA) gene expression was assessed. Consistent with prior studies [5], treatment with a variety of fibrotic and inflammatory mediators (in 1% serum to minimize exogenous growth factors) modulated *Acta2* expression (Table S1). Unexpectedly, none of these mediators modulated *Fap* expression, except ascorbic acid, which promoted *Fap* expression at both the mRNA (Table S1 and Fig. 1A) and protein level (Fig. 1B).

Ascorbic acid (Vitamin C), an essential cofactor for lysyl and prolyl hydroxylation, promotes stable deposition of collagen (Fig. 1C) by ensuring proper folding of its triple

helical structure [34]. Thus, we hypothesized that ascorbic acid regulates FAP expression by promoting ECM deposition. To test this hypothesis, fibroblasts were cultured on FN- and fibrillar collagen-rich fibroblast-derived matrices (FDMs), which had a mean elasticity of 1.5 kPa (Figs. 1D and S1). Interestingly, relative to culture on plastic, fibroblasts cultured on FDMs markedly up-regulated *Fap* gene expression (Fig. 1E). Flow cytometric analysis further demonstrated that culture on FDMs versus plastic enriched for FAP^{Hi} fibroblasts (Fig. 1F). Moreover, a concomitant reduction in αSMA^{Hi} fibroblasts was observed on FDMs versus plastic (Fig. 1F). These data demonstrate that varying substrata can enrich for phenotypically distinct subsets of activated fibroblasts.

1.2.2 ECM composition and elasticity govern activated fibroblast phenotypic heterogeneity

Compared to plastic, FDMs constitute a more physiologically relevant substratum with respect to multiple parameters, including ECM compliance, architecture, and composition [35]. To delineate the roles of ECM elasticity and composition in driving activated fibroblast heterogeneity, we employed polyacrylamide hydrogels (where ECM ligand and elasticity can be independently controlled [36]). We primarily utilized 2 and 20 kilopascal (kPa) hydrogels, which encompasses the range of stiffness found in pathophysiological conditions, including tumors and lung fibrosis [23,24]. Hydrogels were coated with FN or COL I to simulate early versus late stages, respectively, of wound repair, fibrosis, and tumorigenesis [27–29,37].

The elasticity of FN-coated hydrogels impacted fibroblast morphology, with reduced cell spreading and cytoskeletal organization after 72 hours of culture on 2 versus 20 kPa FN-coated hydrogels (Fig. 2A), consistent with previous reports [38,39]. Compared to 20 kPa FN-coated hydrogels, 2 kPa FN-coated hydrogels promoted higher FAP and lower αSMA expression, at the mRNA (Fig. 2B) and protein (Fig. 2C) level. Across the pathophysiological stiffness range, *Fap* gene expression inversely correlated, while *Acta2* gene expression directly correlated with the stiffness of FN-coated hydrogels (Fig. 2D, top panel). The full spectrum of activated fibroblast phenotypic differentiation ($FAP^{Hi}\alpha SMA^{Low}$, $FAP^{Hi}\alpha SMA^{Hi}$, and $FAP^{Low}\alpha SMA^{Hi}$ subsets) was observed on 2, 5, 12, and 20 kPa FN-coated hydrogels, as evidenced by flow cytometric analysis at the single cell level (Fig. 2D, bottom panel). However, our data clearly illustrate a shift in prevalence from the $FAP^{Hi}\alpha SMA^{Low}$ reactive fibroblast phenotype to the $FAP^{Low}\alpha SMA^{Hi}$ myofibroblast phenotype with increasing stiffness (Fig. 2D, bottom panel).

Unlike FN-coated hydrogels, both 2 and 20 kPa COL I-coated hydrogels promoted cell spreading and actin stress fiber formation after 72 hours of culture (Fig. 2A). Moreover, both 2 and 20 kPa COL I-coated hydrogels promoted low *Fap* and high Acta2 gene expression (Fig. 2B), thereby enriching for $FAP^{Low}\alpha SMA^{Hi}$ myofibroblasts (Fig. 2E). Taken together, these data indicate that an integrated response to ECM composition and elasticity governs activated fibroblast heterogeneity.

1.2.3 FAP^{Hi} and αSMA^{Hi} fibroblasts exhibit morphologic and phenotypic plasticity

To assess the potential plasticity of these morphologic and phenotypic fibroblast subsets, we performed serial passage experiments. Specifically, fibroblasts were first cultured on either 2

or 20 kPa FN-coated hydrogels for 72 hours. These cells were recovered and then cultured a second time on either 2 or 20 kPa FN-coated hydrogels for an additional 72 hours.

By phase contrast microscopy, we found that the cell morphology associated with the first culture on 2 versus 20 kPa hydrogels (rounded versus spread cells, respectively) was retained when cultured on hydrogels of the same stiffness for a second time (Fig. 3A). In contrast, cells from 2 kPa hydrogels that were re-cultured on 20 kPa hydrogels displayed a morphology resembling that of cells initially cultured on 20 kPa hydrogels. Similarly, cells cultured on 20 kPa hydrogels that were re-cultured on 2 kPa hydrogels displayed a morphology resembling that of cells initially cultured on 2 kPa hydrogels. Combined, these data suggest that fibroblasts, with respect to their cell morphology, possess the ability to switch phenotypes when changing from soft to stiff substrata, and vice versa. This was further supported by flow cytometric analysis (Fig. 3B): cell populations re-cultured on stiff hydrogels (2 to 20 kPa FN, or 20 to 20 kPa FN) were enriched for αSMA (αSMA^{HI}), showing comparable levels of αSMA to those cells seeded on stiff hydrogels in the first culture (20 kPA FN). Furthermore, the cell populations re-cultured on stiff hydrogels were not enriched for FAP, even when originating from a FAP^{Hi}-enriched population (2 to 20 kPa FN).

1.2.4 Fibroblast differentiation in response to transforming growth factor beta (TGF-β) is governed by ECM composition and elasticity

To dissect the role of growth factors in regulating fibroblast heterogeneity, fibroblasts were cultured in low (1%) serum (to minimize exogenous growth factors) on FN- or COL I-coated hydrogels (2 or 20 kPa) for 72 hours. ECM stiffness regulated *Acta2* expression, even in 1% serum (Fig. 4A). In contrast, *Fap* expression was comparably low in fibroblasts on all substrata in 1% serum (Fig. 4A), unlike in 10% serum (Fig. 2). Serum contains appreciable levels of TGF-β, a pro-fibrotic cytokine thought to promote fibroblast activation. Therefore, we investigated the role of TGF-β-mediated signaling in ECM-dependent regulation of FAP expression by using both gain- and loss-of-function approaches. Addition of recombinant, active TGF-β to 1% serum was sufficient to promote the $FAP^{Hi}\alpha SMA^{Low}$ reactive fibroblast phenotype on 2 kPa FN-coated hydrogels. Conversely, TGF-β promoted the $FAP^{Low}\alpha SMA^{Hi}$ myofibroblast phenotype on 2 kPa COL I-coated hydrogels and 20 kPa hydrogels coated with either FN or COL I (Fig. 4A–B).

To determine whether generation of either activated fibroblast phenotype could be attenuated, fibroblasts in 10% serum were treated with calcipotriol, a vitamin D receptor (VDR) agonist that inhibits TGF-β/SMAD signaling via genomic competition and reverts activated stromal cells to more quiescent phenotypes [40]. The expression of *Cyp24a1*, a VDR target gene, was measured as a positive control for calcipotriol efficacy. Interestingly, calcipotriol induced higher *Cyp24a1* expression in fibroblasts cultured on 2 versus 20 kPa FN-coated hydrogels (Fig. 4C), indicating that high ECM stiffness can confer resistance to calcipotriol. Furthermore, calcipotriol attenuated high *Fap* and *Acta2* gene expression in fibroblasts on 2 and 20 kPa FN-coated hydrogels, respectively (Fig. 4C). These findings demonstrate that VDR agonists can curtail both activated fibroblast phenotypes.

1.2.5 Neither ROCK nor FAK activity are required to induce the FAP^{Hi} reactive fibroblast phenotype

Both Rho kinase (ROCK) and focal adhesion kinase (FAK) activity can promote αSMA^{Hi} myofibroblast differentiation. ROCK activity facilitates the actin cytoskeletal reorganization necessary for myofibroblast differentiation in response to ECM stiffening [41]. FAK activity facilitates TGF-β-induced myofibroblast differentiation [42]. Furthermore, FN-mediated FAK activation depends on stiffness, since exposure of the cryptic FN synergy site requires mechanical tension [43]. Therefore, we assessed whether ROCK or FAK activity similarly regulate FAP^{Hi} reactive fibroblast differentiation. FAP^{Hi} fibroblasts (on 2 kPa FN) and αSMA^{Hi} myofibroblasts (on 20 kPa FN) were treated with a ROCK (Y-27632) or FAK (PF573228) inhibitor. As expected, ROCK inhibition attenuated actin stress fiber formation (Fig. S2A) and *Acta2* expression (Fig. S2B) on 20 kPa FN-coated hydrogels. In contrast, ROCK inhibition had no effect on *Fap* expression on 2 or 20 kPa FN-coated hydrogels (Fig. S2B). Treatment with PF573228 diminished FAK activity, as indicated by reduced phospo-FAK^{Tyr397} levels (Fig. S2C). However, FAK inhibition did not revert either the FAP^{Hi} or αSMA^{Hi} phenotype on 2 or 20 kPa FN, respectively (Fig. S2D). Thus, FAK activity does not appear to be required for the induction of either activated fibroblast phenotype in response to changes in the elasticity of FN-coated hydrogels.

1.2.6 Gene expression profiling indicates that FAP^{Hi} reactive fibroblasts predominantly synthesize and proteolyze ECM, while αSMA^{Hi} myofibroblasts mediate contraction

To identify potentially unique functional roles of fibroblast subsets in tissue remodeling, we compared gene expression profiles of fibroblasts cultured in 10% serum on 2 (enriched for FAP^{Hi} reactive fibroblasts) versus 20 (enriched for αSMA^{Hi} myofibroblasts) kPa FN-coated hydrogels. FAP^{Hi} fibroblasts exhibited a more ECM proteolytic phenotype, with higher gene expression of most matrix metalloproteinases (*Mmps*) and tissue plasminogen activator (*Plat*; Fig. 5A). Meanwhile, gene expression of most tissue inhibitors of metalloproteinases (*Timps*) was comparable or reduced in FAP^{Hi} compared to αSMA^{Hi} fibroblasts (Fig. 5A). FAP^{Hi} fibroblasts also exhibited higher gene expression of many ECM and matricellular constituents, including collagens I (*Col1a1*) and III (*Col3a1*), decorin (*Dcn*), extra domain A FN (*EDA-Fn1*), thrombospondin 2 (*Thbs2*), and osteopontin (*Spp1*; Fig. 5A–B). Notably, αSMA^{Hi} myofibroblasts on 20 kPa (FN- or COL1-coated) and 2 kPa COL 1-coated hydrogels exhibited comparably low gene expression of ECM proteases and components (Fig. S3). Thus, regardless of the stiffness and/or composition of the underlying substratum, αSMA^{Hi} myofibroblasts seem to consistently exhibit a tissue remodeling gene expression signature distinct from that of FAP^{Hi} fibroblasts. Collectively, these results implicate FAP^{Hi} fibroblasts in the dynamic ECM deposition and turnover characteristic of desmoplastic tissue.

On the other hand, FAP^{Hi} fibroblasts showed lower gene expression of constituents of the actomyosin contractile apparatus, such as smooth muscle myosin heavy chain (*Myh11*; Fig. 5B) and beta actin (*Actb*; Fig. 5C). Furthermore, the gene expression of mediators known to promote fibroblast contractility, including caveolin-1 (*Cav1*) and endothelin (*Edn1*), was attenuated in FAP^{Hi} compared to αSMA^{Hi} fibroblasts (Fig. 5C). The reduced gene expression of most integrin subunits in FAP^{Hi} fibroblasts (Fig. 5C) also indicates reduced

contractile capacity, considering the necessity of integrins for fibroblasts to exert contractile force on ECM [25]. The gene expression of lysyl oxidase (*Lox*), an enzyme that crosslinks collagen, was also reduced in FAP^{Hi} fibroblasts (Fig. 5C). Taken together, these results suggest that FAP^{Hi} reactive fibroblasts have a diminished capacity to contract and crosslink ECM compared to αSMA^{Hi} myofibroblasts.

FAP^{Hi} reactive fibroblasts and αSMA^{Hi} myofibroblasts also diverged with respect to their gene expression of growth factors, inflammatory mediators, and regulators of cell cycle progression. Compared to αSMA^{Hi} myofibroblasts, FAP^{Hi} fibroblasts expressed lower mRNA levels of autocrine growth factors that can promote myofibroblast differentiation and expansion, including connective tissue growth factor (*Ctgf*), platelet derived growth factor α (*Pdgfa*), *Tgfb2*, and *Tgfb3* (Fig. 5D). Conversely, FAP^{Hi} fibroblasts expressed higher mRNA levels of hepatocyte growth factor (*Hgf*), a paracrine growth factor known to promote epithelial proliferation and survival (Fig. 5D). FAP^{Hi} fibroblasts also expressed higher mRNA levels of most inflammatory mediators assessed in our fibrosis array, however, they were expressed at low levels, exhibited relatively high variability, and did not achieve statistical significance at a confidence level of 95% (Table S2). Lastly, FAP^{Hi} fibroblasts exhibited lower gene expression of pro-proliferative transcription factors, such as jun oncogene (*Jun;* Fig. 5D) and myelocytomatosis oncogene (*Myc*; Fig. 5D), and mediators of cell cycle progression, such as cyclin A2 (*Ccna2*; Fig. 5B), suggestive of a less proliferative phenotype.

We then performed functional assays to corroborate the unique functionality of αSMA^{Hi} and FAP^{Hi} fibroblasts indicated by gene expression profiling. Assessment of cellular gelatinase activity using DQ gelatin demonstrated that FAP^{Hi} fibroblasts exhibited higher gelatinase activity than αSMA^{Hi} myofibroblasts (Figs. 5E and S4). Furthermore, atomic force microscopy demonstrated that FAP^{Hi} fibroblasts exhibit lower intracellular tension than αSMA^{Hi} myofibroblasts (Fig. 5F). Taken together with our gene expression data, these results further suggest that FAP^{Hi} fibroblasts display a more highly ECM proteolytic phenotype than the more highly contractile αSMA^{Hi} myofibroblasts.

1.3 Discussion

In summary, we delineated features of remodeling tissues that direct activated fibroblast heterogeneity. In our proposed model (Fig. 6), a convergence of ECM composition, elasticity, and TGF-β signaling governs FAP^{Hi}αSMA^{Low}, FAP^{Hi}αSMA^{Hi}, and FAP^{Low}αSMA^{Hi} fibroblast phenotypic heterogeneity. These data help explain the activated fibroblast heterogeneity observed *in vivo*, where FAP and αSMA identify distinct, yet overlapping, fibroblast subsets. This heterogeneity likely stems from the spatiotemporally dynamic variation in ECM composition and elasticity in injury, fibrosis, and cancer [21–26,28]. Furthermore, our data from gene expression profiling and functional tests indicate potentially unique functionality of these fibroblast subsets in tissue remodeling. FAP^{Hi} reactive fibroblasts exhibited an ECM synthetic and proteolytic phenotype, while αSMA^{Hi} myofibroblasts exhibited a contractile and proliferative phenotype.

Extrapolating our model to the well-characterized progression of acute injury resolution [22] illuminates ECM-dependent regulation and diverse functionality of fibroblast subsets in tissue remodeling. In early wounds, the highly elastic, FN-rich environment likely promotes FAP^{Hi} fibroblast differentiation. The gene expression and functional profile of FAP^{Hi} fibroblasts suggests that they orchestrate early phases of wound resolution by secreting: (1) ECM proteases to facilitate cell migration into the wound, (2) paracrine growth factors to support re-epithelialization, and (3) ECM and matricellular components to replace provisional ECM with COL 1-rich connective tissue. Thereafter, the stiff, COL 1-rich environment of late granulation tissue likely promotes αSMA^{Hi} myofibroblast differentiation. The gene expression and functional profile of αSMA^{Hi} myofibroblasts suggests that they orchestrate late phases of wound resolution, including fibro-proliferation (via secretion of autocrine growth factors) and wound closure (via contraction). We are now conducting studies utilizing murine models of tissue injury to assess this proposed model of temporal regulation and diverse functionality of FAP^{Hi} and αSMA^{Hi} fibroblasts in wound resolution.

Comparable regulation and functionality of FAP^{Hi} and αSMA^{Hi} fibroblast subsets likely occur in tumors, considering the parallels between the wound healing response and tumorigenesis [27–29]. Previous studies have characterized diverse mechanisms by which carcinoma-associated fibroblasts promote tumor growth. However, the diverse roles of fibroblast subsets in tumorigenesis remained unclear. Our gene expression and functional analysis suggests that FAP^{Hi} and αSMA^{Hi} fibroblasts diverge in their tumor-promoting functions. For example, αSMA^{Hi} myofibroblasts express higher mRNA levels of *Lox*, an enzyme that stiffens ECM by crosslinking collagen, which promotes focal adhesions, PI3K signaling, and consequently, tumor invasion [44]. αSMA^{Hi} myofibroblasts also exhibit higher gene expression of *Cav1*, which promotes Rho-dependent contraction, ECM alignment and stiffening, and consequently, tumor invasion [45]. Meanwhile, FAP^{Hi} fibroblasts exhibit higher gene expression of many tumor-promoting ECM proteases, including *Fap* itself and most *Mmps*. Extensive research has previously demonstrated fundamental roles of these stromal proteases in tumor invasion [46], angiogenesis [47,48], proliferation [47,49,50], and epithelial-mesenchymal transition [51,52]. Moreover, compared to αSMA^{Hi} myofibroblasts, FAP^{Hi} fibroblasts exhibit higher gene expression of *Hgf*, a previously described mechanism by which stromal fibroblasts promote oncogenesis and resistance to targeted cancer therapies [53,54].

Importantly, our study addresses the ongoing controversy regarding intratumoral fibroblasts as therapeutic targets [55,56]. A number of laboratories have employed diverse approaches to deplete FAP^{Hi} fibroblasts in murine tumor models [11,20,57–62]. Virtually all these studies illustrated that depletion of FAP^{Hi} fibroblasts disrupts desmoplastic stroma and impedes tumor progression, corroborating the data presented herein and the correlation between high FAP expression and poor prognosis in myriad solid tumor types [63–79]. On the contrary, the net effect of αSMA^{Hi} myofibroblasts in tumor progression remains obfuscated due to conflicting reports. Although many studies have demonstrated a pro-tumorigenic role for αSMA^{Hi} myofibroblasts[80,81], one recent study utilizing αSMA-thymidine kinase transgenic mice demonstrated that depletion of proliferating αSMA^{Hi} myofibroblasts (via systemic ganciclovir administration) accelerated pancreatic ductal

adenocarcinoma aggressiveness [15]. Importantly, αSMA^{Hi} myofibroblast depletion did not diminish the prevalence of FAP^{Hi} fibroblasts [15], a population that possesses unique tumor-promoting capabilities. In contrast, FAP^{Hi} fibroblast depletion also eliminated most intratumoral αSMA^{Hi} myofibroblasts [11]. Thus, FAP^{Hi} fibroblast depletion may have demonstrated superior anti-tumor efficacy than αSMA^{Hi} myofibroblast depletion because it eliminated heterogeneous, tumor-promoting populations of activated fibroblasts. Alternately, the net benefit of FAP^{Hi} fibroblast depletion may have overcome the potential detrimental effect of αSMA^{Hi} myofibroblast depletion. Our results from serial passage experiments suggest that FAP^{Hi} and αSMA^{Hi} fibroblasts exhibit morphologic and phenotypic plasticity. However, future studies should further investigate the lineage, interdependence, and plasticity of these activated fibroblast subsets *in vivo*. FAP^{Hi} fibroblasts may facilitate the generation and/or recruitment of αSMA^{Hi} myofibroblasts, or myofibroblast precursors may express FAP.

Unraveling the complex regulation of fibroblast heterogeneity will hasten the successful application of therapies that target fibroblasts. In fact, our findings may help explain recent failures in clinical trials of a few molecularly targeted approaches. For example, simtuzumab (an antibody that blocks LOXL2 enzymatic activity) failed in clinical trials for colorectal adenocarcinoma [82], metastatic pancreatic adenocarcinoma[83], and idiopathic pulmonary fibrosis [84,85]. The clinical use of simtuzumab aimed to curb tumor and fibrosis progression by reducing ECM stiffness and myofibroblast generation. Our finding that FAP^{Hi} fibroblasts prevail at low stiffness might help explain the inefficacy of simtuzumab, considering the tumor- and fibrosis-promoting propensities of FAP^{Hi} fibroblasts. The attenuation of myofibroblast generation via inhibitors of sonic hedgehog signaling may have failed in clinical trials for similar reasons [86–88]. Intriguingly, calcipotriol-mediated blockade of TGF-β/SMAD signaling (currently being evaluated in clinical trials) has shown promise in pre-clinical models of both pancreatic ductal adenocarcinoma and liver cirrhosis [40,89]. We have now demonstrated that calcipotriol can attenuate fibroblast activation to both the FAP^{Hi} and αSMA^{Hi} phenotype, which helps explain the efficacy of calcipotriol in treating both fibrosis and cancer. Overall, our findings underscore the importance of comprehensive monitoring of heterogenous fibroblast populations in response to stroma-targeted therapies to identify optimal treatment modalities.

1.4 Methods

1.4.1 Isolation of murine lung fibroblasts

Lungs were harvested from 10- to 16-week-old male or female C57BL/6 (Charles River) mice. Lungs were finely minced, then digested in a cocktail of collagenases I, II, and IV (Worthington; each at 250 μg/ml in DMEM) at 37°C for 2 hours. The collagenase solution was quenched with an equivalent volume of 10% heat-inactivated fetal calf serum (FCS) DMEM. The digested tissue was sequentially strained through 70 and 40 μm cell strainers then spun at 1200 r.p.m. for 10 minutes at 4°C. The cell pellet was re-suspended in 10% FCS DMEM (containing HEPES, L-glutamine, penicillin-streptomycin, fungizone, and gentamicin) and plated on tissue culture-treated plastic (polystyrene). Cells were maintained at 37°C with 5% CO_2 in a humidified incubator. The next day, cell monolayers were washed

several times with PBS to remove non-adherent cells. Cells were maintained in 10% FCS DMEM on tissue culture-treated plastic for two passages. Second passage fibroblasts were used for all experiments.

1.4.2 Fibroblast-derived matrices (FDMs)

Decellularized FDMs were generated as described previously [90], using murine lung fibroblasts cultured at confluence in the presence of 75 μg/ml ascorbic acid for 8 days.

1.4.3 Hydrogels

Polyacrylamide hydrogels of varying stiffness were prepared and coated overnight at 4°C with bovine FN (EMD Millipore; 5 μg/ml) or COL I (PureCol; Advanced BioMatrix; 10 μg/ml) as described previously [36]. Hydrogels were rinsed twice with PBS and unreacted N-hydroxysuccinimide was blocked with 1 mg/ml heat-inactivated bovine serum albumin in serum-free DMEM for 30 minutes at 37°C. Hydrogels were rinsed twice with PBS before cell seeding.

1.4.4. RNA isolation and quantitative real-time polymerase chain reaction (qRT-PCR)

Cells were rinsed with PBS, lysed in 1 ml Trizol (Invitrogen), and processed for RNA extraction according to manufacturer's instructions. After quality assessment by agarose gel electrophoresis, reverse transcription was performed following the standard protocol for the TaqMan Reverse Transcription kit (Applied Biosystems). Transcript levels were assayed via the StepOnePlus Real-Time PCR System (Applied Biosystems) using SYBR Green (Invitrogen). mRNA levels for all genes of interest were normalized to *Hprt1* mRNA levels. Primer sequences: *Fap*-F, 5'-cacctgatcggcaatttgtg; *Fap*-R, 5'-cccattctgaaggtcgtagatgt; *Acta2*-F, 5'-ccagagcaagagagggatcct; *Acta2*-R, 5'-tgtcgtcccagttggtgatg; *Hprt1*-F, 5'-tgacactggtaaaacaatgca; *Hprt1*-R, 5'-ggtccttttcaccagcaagct; *Tnc*-F, 5'-ggacttacgggtgtctgaaacc; *Tnc*-R, 5'-tgaggcggtaacgatcaaact; *Cyp24a1*-F, 5'-ccagcggctagagatcaaac; *Cyp24a1*-R, 5'-cacgggcttcatgagtttct; *Spp1*-F, 5'-ccctcgatgtcatccctgtt; *Spp1*-R, 5'-tgccctttccgttgttgtc; *Myh11*-F, 5'-gacaactcctctcgctttgg; *Myh11*-R, 5'-gctctccaaaagcaggtcac; *Ccna2*-F, 5'-tggatggcagttttgaatcacc; *Ccna2*-R, 5'-ccctaaggtacgtgtgaatgtc; *EDA-Fn1*-F, 5'-cgagccctgaggatggaat; *EDA-Fn1*-R, 5'-agctctgcagtgtcgtcttcac; *Has2*-F, 5'-cggtcgtctcaaattcatctg; *Has2*-R, 5'-acaatgcatcttgttcagctc; *Col1a1*-F, 5'-cccaaggaaaagaagcacgtc; *Col1a1*-R, 5'-acattaggcgcaggaaggtca; *Col3a1*-F, 5'-gaaagagtggtgacagaggag; *Col3a1-R, 5'*-tgatgccattagagccacg; *Mmp2*-F*, 5'*-cccatgaagccttgtttacca; *Mmp2*-R, 5'-tggaagcggaacgggaact.

1.4.5 Fibrosis gene expression array

RNA was extracted as described above. RNA purification was performed following the standard protocol for the RNeasy Mini Kit with on-column DNase digestion (Qiagen). After quality assessment by agarose gel electrophoresis, cDNA was synthesized (using 1 μg RNA per sample) with the RT^2 First Strand Kit (Qiagen). Both RNA and cDNA quality were confirmed using the Murine RT^2 Profiler Quality Control Array (Qiagen). Transcript levels were assessed with the RT^2 Profiler Mouse Fibrosis PCR Array (Qiagen) using RT^2 Sybr

Green ROX qPCR Mastermix (Qiagen). RNA levels for all genes of interest were normalized to β_2 microglobulin (β_2M) mRNA levels.

1.4.6 Flow cytometry

For hydrogel (Figs. 2–4) and Vit. C (Fig 1B) experiments, cells were trypsinized to obtain a single cell suspension. For FDM experiments (Fig. 1F), cells (on plastic or FDM) were trypsinized, and then incubated with 500 μg/ml collagenase I (Worthington) for 30 minutes at 37°C to obtain a single cell suspension. Flow cytometric analyses were performed on an LSR-Fortessa using FACSDiva software (BD Bioscience) and data were analyzed using FlowJo (Tree Star).

1.4.7 Antibodies used for flow cytometry

Biotinylated anti-FAP (Clone 73-3) antibody was generated in-house, and detected using Streptavidin-APC (BioLegend). The specificity of the anti-FAP antibody was verified based on reactivity with cells from wild-type but not FAP-null mice. Dead cells were excluded by using the Live/Dead Fixable Violet Dead Cell Stain Kit (Molecular Probes). Staining with anti-αSMA antibody (Sigma, clone1A4, FITC) was performed after permeabilizing cell suspensions with the Cytofix/Cytoperm Fixation/Permeabilization Kit (BD Biosciences), as per the manufacturer's instructions.

1.4.8 Treatment with inhibitors or soluble factors

For indicated experiments, cells were treated with recombinant human active TGF-β (R&D), PF573228 (Tocris), Y-27632 (Sigma), calcipotriol (Tocris), L-ascorbic acid (Vit. C; Fisher), basic fibroblast growth factor (bFGF; Peprotech), interleukin (IL)-1β (Peprotech), IL-3 (Peprotech), interferon gamma (IFNγ; R&D), IL-6 (Peprotech), tumor necrosis factor alpha (TNFα; Peprotech), high molecular weight hyaluronan (HMW HA; Healon), low molecular weight hyaluronan (LMW HA; ICN Biochemicals), periostin/OSF-2 (R&D), buthionine-sulfoximine (BSO; Sigma), tiron (Sigma), trichostatin A (Sigma), pleiotrophin (R&D), angiotensin II (Sigma), and platelet-derived growth factor-bb (PDGFbb; Calbiochem).

1.4.9 Immunoblot

Total cell lysates were prepared from fibroblasts cultured on hydrogels by placing coverslips face down on 4X NuPAGE LDS Sample Buffer (Invitrogen; supplemented with 10 mM 2-mercaptoethanol) for 2 minutes. Cell lysates were then heated at 70°C for 10 minutes. Equal amounts of extracted protein were resolved on NuPAGE 4–12% Bis-Tris gels (Invitrogen) and the fractioned proteins were transferred onto PVDF membranes. Membranes were probed with antibodies to FAK (Cell Signaling, 3285) and phospo-FAK^{Tyr397} (Cell Signaling, 3283), followed by HRP-conjugated goat anti-rabbit secondary antibody (Sigma, A0545).

1.4.10 Microscopy

Imaging of fibrillar collagen in decellularized fibroblast-derived matrices was based on second harmonic generation utilizing a Leica SP5 confocal/multiphoton microscope (Leica

Microsystems) at 20X magnification, as described previously[91]. Immunofluorescent (IF) and phase contrast images were obtained with a Nikon Eclipse Ti-E inverted microscope at 10X (FN, phase contrast) or 20X (phalloidin; DQ gelatin, phase contrast) magnification.

1.4.11 Hydroxyproline assay

Collagen content in FDMs produced by lung fibroblasts (in the presence or absence of 75 μg/ml ascorbic acid) was quantified by measuring hydroxyproline levels (normalized to cell number as measured by calcein AM levels), as previously described[92].

1.4.12 IF

For FN IF, FDMs produced by lung fibroblasts were incubated with rabbit anti-FN antibody (Sigma, Clone F3648), followed by Alexa Fluor 658 goat anti-rabbit antibody (Invitrogen). For visualization of the actin cytoskeleton, lung fibroblasts on 2 and 20 kPa hydrogels were fixed with 4% paraformaldehyde, permeabilized with 0.1% Triton-X-100, then stained with Alexa Fluor 594-conjugated phalloidin (Molecular Probes) and DAPI.

1.4.13 Atomic Force Microscopy

The elastic moduli of cells, FDMs, and hydrogels were measured using a Catalyst Bioscope AFM mounted on a Nikon Eclipse TE 200 microscope. Samples were indented with a standard silicon nitride cantilever (spring constant =0.07 N/m) with a 1 μm spherical tip using a maximum force of 7 nN. AFM force curves were analyzed by fitting the sample indentation to the Hertz model for a sphere making contact with a homogeneous elastic half space. Three measurements of intracellular stiffness were collected at regions of the cell between the nucleus and the periphery, and ten cells were measured per condition. AFM force curves were analyzed and converted to Young's modulus using NanoScope Analysis software from Bruker.

1.4.14 Gelatinolysis Assay

Cells were seeded onto 2 or 20 kPa FN-coated hydrogels and incubated for 48 hours. Growth medium was then removed and replaced with a 1:1 ratio of growth medium:reaction buffer (50 mM Tris, 150 mM NaCl, 5 mM $CaCl_2$, 0.2 mM NaN_3) containing 20 μg/ml DQ gelatin (D12054, Thermofisher). Cells were incubated for a further 24 hours before being fixed with 4% paraformaldehyde, and counter-stained with DAPI. Hydrogels were imaged in phase contrast / fluorescence at 20x magnification. DQ intensity levels were analyzed using NIS Elements software as follows: integrated fluorescent intensity levels for DQ gelatin were calculated per cell (150 cells per group; 2 groups per experiment; 3 independent experiments). Mean relative DQ intensities per cell area were then calculated for the 3 independent experiments.

1.4.15 Statistics

All results are reported as mean (of the indicated number of independent experiments) +/− standard error of the mean (SEM). Statistical analysis was performed using one-way analysis of variance (ANOVA) with the Tukey's multiple comparison test or two-tailed

Student's *t* test (Prism 7.0, GraphPad Software). Asterisks denote statistical significance: **** $p < 0.0001$, *** $p < 0.001$, ** $p < 0.01$, * $p < 0.05$.

Acknowledgments

We thank the Biomechanics Core Facility of the Institute for Translational Medicine and Therapeutics (ITMAT) for providing hydrogels and performing atomic force microscopy, and the Shared Matrix Analysis Facility of the Penn Vet Cancer Center for technical support. We also thank Dr. Rebecca Wells and Dr. Sandra Ryeom for helpful discussions and assistance in preparing the manuscript. The authors declare no competing financial interests.

1.6 Funding

This work was supported by the National Institute of Health (grant numbers: R01CA141144, R21CA169741, and R01CA172921 (EP)).

Abbreviations

AFM	atomic force microscopy
αSMA	alpha-smooth muscle actin
COL 1	collagen I
ECM	extracellular matrix
FAK	focal adhesion kinase
FAP	fibroblast activation protein
FDM	fibroblast-derived matrix
FN	fibronectin
kPa	kilopascal
ROCK	rho kinase
TGF-β	transforming growth factor beta

1.7 References

1. Servais C, Erez N. From sentinel cells to inflammatory culprits: cancer-associated fibroblasts in tumour-related inflammation. J Pathol. 2013; 229:198–207. DOI: 10.1002/path.4103 [PubMed: 22996812]
2. Tomasek JJ, Gabbiani G, Hinz B, Chaponnier C, Brown RA. Myofibroblasts and mechano-regulation of connective tissue remodelling. Nat Rev Mol Cell Biol. 2002; 3:349–363. http://dx.doi.org/10.1038/nrm809. [PubMed: 11988769]
3. Hinz B, Phan SH, Thannickal VJ, Prunotto M, Desmoulière A, Varga J, De Wever O, Mareel M, Gabbiani G. Recent developments in myofibroblast biology: paradigms for connective tissue remodeling. Am J Pathol. 2012; 180:1340–1355. DOI: 10.1016/j.ajpath.2012.02.004 [PubMed: 22387320]
4. Hinz B, Phan SH, Thannickal VJ, Galli A, Bochaton-Piallat M-L, Gabbiani G. The myofibroblast: one function, multiple origins. Am J Pathol. 2007; 170:1807–1816. DOI: 10.2353/ajpath.2007.070112 [PubMed: 17525249]
5. Serini G, Gabbiani G. Mechanisms of myofibroblast activity and phenotypic modulation. Exp Cell Res. 1999; 250:273–283. DOI: 10.1006/excr.1999.4543 [PubMed: 10413583]

6. Tillmanns J, Hoffmann D, Habbaba Y, Schmitto JD, Sedding D, Fraccarollo D, Galuppo P, Bauersachs J. Fibroblast activation protein alpha expression identifies activated fibroblasts after myocardial infarction. J Mol Cell Cardiol. 2015; 87:194–203. DOI: 10.1016/j.yjmcc.2015.08.016 [PubMed: 26319660]
7. Acharya PS, Zukas A, Chandan V, Katzenstein ALA, Puré E. Fibroblast activation protein: a serine protease expressed at the remodeling interface in idiopathic pulmonary fibrosis. Hum Pathol. 2006; 37:352–360. DOI: 10.1016/j.humpath.2005.11.020 [PubMed: 16613331]
8. Levy MT, McCaughan GW, Abbott CA, Park JE, Cunningham AM, Müller E, Rettig WJ, Gorrell MD. Fibroblast activation protein: a cell surface dipeptidyl peptidase and gelatinase expressed by stellate cells at the tissue remodelling interface in human cirrhosis. Hepatology. 1999; 29:1768–78. DOI: 10.1002/hep.510290631 [PubMed: 10347120]
9. Bauer S, Jendro MC, Wadle A, Kleber S, Stenner F, Dinser R, Reich A, Faccin E, Gödde S, Dinges H, Müller-Ladner U, Renner C. Fibroblast activation protein is expressed by rheumatoid myofibroblast-like synoviocytes. Arthritis Res Ther. 2006; 8:R171.doi: 10.1186/ar2080 [PubMed: 17105646]
10. Garin-Chesa P, Old LJ, Rettig WJ. Cell surface glycoprotein of reactive stromal fibroblasts as a potential antibody target in human epithelial cancers. Proc Natl Acad Sci U S A. 1990; 87:7235–7239. DOI: 10.1073/pnas.87.18.7235 [PubMed: 2402505]
11. Lo A, Wang L-CS, Scholler J, Monslow J, Avery D, Newick K, O9Brien S, Evans RA, Bajor DJ, Clendenin C, Durham AC, Buza EL, Vonderheide RH, June CH, Albelda SM, Puré E. Tumor-promoting desmoplasia is disrupted by depleting FAP-expressing stromal cells. Cancer Res. 2015; 75:2800–2810. http://cancerres.aacrjournals.org/content/75/14/2800.abstract. [PubMed: 25979873]
12. Tchou J, Zhang PJ, Bi Y, Satija C, Marjumdar R, Stephen TL, Lo A, Chen H, Mies C, June CH, Conejo-Garcia J, Puré E. Fibroblast activation protein expression by stromal cells and tumor-associated macrophages in human breast cancer. Hum Pathol. 2013; 44:2549–2557. DOI: 10.1016/j.humpath.2013.06.016 [PubMed: 24074532]
13. Park JE, Lenter MC, Zimmermann RN, Garin-Chesa P, Old LJ, Rettig WJ. Fibroblast activation protein, a dual specificity serine protease expressed in reactive human tumor stromal fibroblasts. J Biol Chem. 1999; 274:36505–36512. DOI: 10.1074/jbc.274.51.36505 [PubMed: 10593948]
14. Busek P, Balaziova E, Matrasova I, Hilser M, Tomas R, Syrucek M, Zemanova Z, Krepela E, Belacek J, Sedo A. Fibroblast activation protein alpha is expressed by transformed and stromal cells and is associated with mesenchymal features in glioblastoma. Tumor Biol. 2016; 37:13961–13971. DOI: 10.1007/s13277-016-5274-9
15. Özdemir BC, Pentcheva-Hoang T, Carstens JL, Zheng X, Wu CC, Simpson TR, Laklai H, Sugimoto H, Kahlert C, Novitskiy SV, De Jesus-Acosta A, Sharma P, Heidari P, Mahmood U, Chin L, Moses HL, Weaver VM, Maitra A, Allison JP, LeBleu VS, Kalluri R. Depletion of carcinoma-associated fibroblasts and fibrosis induces immunosuppression and accelerates pancreas cancer with reduced survival. Cancer Cell. 2014; 25:719–734. DOI: 10.1016/j.ccr.2014.04.005 [PubMed: 24856586]
16. Öhlund D, Handly-Santana A, Biffi G, Elyada E, Almeida AS, Ponz-Sarvise M, Corbo V, Oni TE, Hearn SA, Lee EJ, Chio IIC, Hwang C-I, Tiriac H, Baker LA, Engle DD, Feig C, Kultti A, Egeblad M, Fearon DT, Crawford JM, Clevers H, Park Y, Tuveson DA. Distinct populations of inflammatory fibroblasts and myofibroblasts in pancreatic cancer. J Exp Med. 2017; 214:579–596. http://jem.rupress.org/content/early/2017/02/23/jem.20162024.abstract. [PubMed: 28232471]
17. Kilvaer TK, Khanehkenari MR, Hellevik T, Al-Saad S, Paulsen EE, Bremnes RM, Busund LT, Donnem T, Martinez IZ. Cancer associated fibroblasts in stage I-IIIA NSCLC: prognostic impact and their correlations with tumor molecular markers. PLoS One. 2015; 10:e0134965.doi: 10.1371/journal.pone.0134965 [PubMed: 26252379]
18. Yang X, Lin Y, Shi Y, Li B, Liu W, Yin W, Dang Y, Chu Y, Fan J, He R. FAP promotes immunosuppression by cancer-associated fibroblasts in the tumor microenvironment via STAT3–CCL2 signaling. Cancer Res. 2016; 76:4124 LP–4135. http://cancerres.aacrjournals.org/content/76/14/4124.abstract. [PubMed: 27216177]
19. Kraman M, Bambrough PJ, Arnold JN, Roberts EW, Magiera L, Jones JO, Gopinathan A, Tuveson DA, Fearon DT. Suppression of antitumor immunity by stromal cells expressing fibroblast

activation protein–α. Science. 2010; 330:827–830. http://science.sciencemag.org/content/330/6005/827.abstract. [PubMed: 21051638]

20. Wang L-CS, Lo A, Scholler J, Sun J, Majumdar RS, Kapoor V, Antzis M, Cotner CE, Johnson LA, Durham AC, Solomides CC, June CH, Puré E, Albelda SM. Targeting fibroblast activation protein in tumor stroma with chimeric antigen receptor T cells can inhibit tumor growth and augment host immunity without severe toxicity. Cancer Immunol Res. 2014; 2:154 LP–166. http://cancerimmunolres.aacrjournals.org/content/2/2/154.abstract. [PubMed: 24778279]
21. Hurme T, Kalimo H, Sandberg M, Lehto M, Vuorio E. Localization of type I and III collagen and fibronectin production in injured gastrocnemius muscle. Lab Invest. 1991; 64:76–84. http://europepmc.org/abstract/MED/1703587. [PubMed: 1703587]
22. Singer AJ, Clark RAF. Cutaneous wound healing. N Engl J Med. 1999; 341:738–746. DOI: 10.1056/NEJM199909023411006 [PubMed: 10471461]
23. Liu F, Mih JD, Shea BS, Kho AT, Sharif AS, Tager AM, Tschumperlin DJ. Feedback amplification of fibrosis through matrix stiffening and COX-2 suppression. J Cell Biol. 2010; 190:693–706. http://jcb.rupress.org/content/190/4/693.abstract. [PubMed: 20733059]
24. Plodinec M, Loparic M, Monnier CA, Obermann EC, Zanetti-Dallenbach R, Oertle P, Hyotyla JT, Aebi U, Bentires-Alj M, LYH, Schoenenberger C-A. The nanomechanical signature of breast cancer. Nat Nano. 2012; 7:757–765. http://dx.doi.org/10.1038/nnano.2012.167.
25. Yu H, Mouw JK, Weaver VM. Forcing form and function: biomechanical regulation of tumor evolution. Trends Cell Biol. 2011; 21:47–56. DOI: 10.1016/j.tcb.2010.08.015 [PubMed: 20870407]
26. Kubow KE, Vukmirovic R, Zhe L, Klotzsch E, Smith ML, Gourdon D, Luna S, Vogel V. Mechanical forces regulate the interactions of fibronectin and collagen I in extracellular matrix. Nat Commun. 2015; 6:8026.doi: 10.1038/ncomms9026 [PubMed: 26272817]
27. Dvorak HF. Tumors: wounds that do not heal--Redux. Cancer Immunol Res. 2015; 3:1–11. DOI: 10.1158/2326-6066.CIR-14-0209 [PubMed: 25568067]
28. Dvorak HF. Tumors: wounds that do not heal. N Engl J Med. 1986; 315:1650–1659. DOI: 10.1056/NEJM198612253152606 [PubMed: 3537791]
29. Schafer M, Werner S. Cancer as an overhealing wound: an old hypothesis revisited. Nat Rev Mol Cell Biol. 2008; 9:628–638. http://dx.doi.org/10.1038/nrm2455. [PubMed: 18628784]
30. Goffin JM, Pittet P, Csucs G, Lussi JW, Meister JJ, Hinz B. Focal adhesion size controls tension-dependent recruitment of alpha-smooth muscle actin to stress fibers. J Cell Biol. 2006; 172:259–68. DOI: 10.1083/jcb.200506179 [PubMed: 16401722]
31. Öhlund D, Elyada E, Tuveson D. Fibroblast heterogeneity in the cancer wound. J Exp Med. 2014; 211:1503–1523. http://jem.rupress.org/content/211/8/1503.abstract. [PubMed: 25071162]
32. Kalluri R. The biology and function of fibroblasts in cancer. Nat Rev Cancer. 2016; 16:582–598. http://dx.doi.org/10.1038/nrc.2016.73. [PubMed: 27550820]
33. Puré E, Lo A. Can targeting stroma pave the way to enhanced antitumor immunity and immunotherapy of solid tumors? Cancer Immunol Res. 2016; 4:269–278. http://cancerimmunolres.aacrjournals.org/content/4/4/269.abstract. [PubMed: 27036971]
34. Pinnell SR. Regulation of collagen biosynthesis by ascorbic acid: a review. Yale J Biol Med. 1985; 58:553–559. http://www.ncbi.nlm.nih.gov/pmc/articles/PMC2589959/. [PubMed: 3008449]
35. Cukierman E, Pankov R, Stevens DR, Yamada KM. Taking cell-matrix adhesions to the third dimension. Science. 2001; 294:1708–1712. http://science.sciencemag.org/content/294/5547/1708.abstract. [PubMed: 11721053]
36. Cretu A, Castagnino P, Assoian R. Studying the effects of matrix stiffness on cellular function using acrylamide-based hydrogels. J Vis Exp. 2010; :2089.doi: 10.3791/2089 [PubMed: 20736914]
37. Rybinski B, Franco-Barraza J, Cukierman E. The wound healing, chronic fibrosis, and cancer progression triad. Physiol Genomics. 2014; 46:223–244. DOI: 10.1152/physiolgenomics.00158.2013 [PubMed: 24520152]
38. Solon J, Levental I, Sengupta K, Georges PC, Janmey PA. Fibroblast adaptation and stiffness matching to soft elastic substrates. Biophys J. 2007; 93:4453–4461. DOI: 10.1529/biophysj.106.101386 [PubMed: 18045965]

39. Klein EA, Castagnino P, Kothapalli D, Yin L, Byfield FJ, Xu T, Levental I, Hawthorne E, Janmey PA, Assoian RK. Cell cycle control by physiological matrix elasticity and in vivo tissue stiffening. Curr Biol. 2009; 19:1511–1518. DOI: 10.1016/j.cub.2009.07.069 [PubMed: 19765988]
40. Ding N, Yu RT, Subramaniam N, Sherman MH, Wilson C, Rao R, Leblanc M, Coulter S, He M, Scott C, Lau SL, Atkins AR, Barish GD, Gunton JE, Liddle C, Downes M, Evans RM. A vitamin D receptor/SMAD genomic circuit gates hepatic fibrotic response. Cell. 2013; 153:601–613. DOI: 10.1016/j.cell.2013.03.028 [PubMed: 23622244]
41. Huang X, Yang N, Fiore VF, Barker TH, Sun Y, Morris SW, Ding Q, Thannickal VJ, Zhou Y. Matrix stiffness induced myofibroblast differentiation is mediated by intrinsic mechanotransduction. Am J Respir Cell Mol Biol. 2012; 47:340–348. DOI: 10.1165/rcmb.2012-0050OC [PubMed: 22461426]
42. Thannickal VJ, Lee DY, White ES, Cui Z, Larios JM, Chacon R, Horowitz JC, Day RM, Thomas PE. Myofibroblast differentiation by transforming growth factor-beta1 is dependent on cell adhesion and integrin signaling via focal adhesion kinase. J Biol Chem. 2003; 278:12384–12389. DOI: 10.1074/jbc.M208544200 [PubMed: 12531888]
43. Seong J, Tajik A, Sun J, Guan JL, Humphries MJ, Craig SE, Shekaran A, García AJ, Lu S, Lin MZ, Wang N, Wang Y. Distinct biophysical mechanisms of focal adhesion kinase mechanoactivation by different extracellular matrix proteins. Proc Natl Acad Sci. 2013; 110:19372–19377. DOI: 10.1073/pnas.1307405110 [PubMed: 24222685]
44. Levental KR, Yu H, Kass L, Lakins JN, Egeblad M, Erler JT, Fong SFT, Csiszar K, Giaccia A, Weninger W, Yamauchi M, Gasser DL, Weaver VM. Matrix crosslinking forces tumor progression by enhancing integrin signaling. Cell. 2009; 139:891–906. DOI: 10.1016/j.cell.2009.10.027 [PubMed: 19931152]
45. Goetz JG, Minguet S, Navarro-Lérida I, Lazcano JJ, Samaniego R, Calvo E, Tello M, Osteso-Ibáñez T, Pellinen T, Echarri A, Cerezo A, Klein-Szanto AJP, Garcia R, Keely PJ, Sánchez-Mateos P, Cukierman E, Del Pozo MA. Biomechanical remodeling of the microenvironment by stromal Caveolin-1 favors tumor invasion and metastasis. Cell. 2011; 146:148–163. DOI: 10.1016/j.cell.2011.05.040 [PubMed: 21729786]
46. Boire A, Covic L, Agarwal A, Jacques S, Sherifi S, Kuliopulos A. PAR1 is a matrix metalloprotease-1 receptor that promotes invasion and tumorigenesis of breast cancer cells. Cell. 2005; 120:303–313. DOI: 10.1016/j.cell.2004.12.018 [PubMed: 15707890]
47. Santos AM, Jung J, Aziz N, Kissil JL, Puré E. Targeting fibroblast activation protein inhibits tumor stromagenesis and growth in mice. J Clin Invest. 2009; 119:3613–3625. DOI: 10.1172/JCI38988 [PubMed: 19920354]
48. Itoh T, Tanioka M, Yoshida H, Yoshioka T, Nishimoto H, Itohara S. Reduced angiogenesis and tumor progression in gelatinase A-deficient mice. Cancer Res. 1998; 58:1048–1051. http://cancerres.aacrjournals.org/content/58/5/1048.abstract. [PubMed: 9500469]
49. Cheng JD, Dunbrack RL, Valianou M, Rogatko A, Alpaugh RK, Weiner LM. Promotion of tumor growth by murine fibroblast activation protein, a serine protease, in an animal model. Cancer Res. 2002; 62:4767–4772. [PubMed: 12183436]
50. Cheng JD, Valianou M, Canutescu AA, Jaffe EK, Lee HO, Wang H, Lai JH, Bachovchin WW, Weiner LM. Abrogation of fibroblast activation protein enzymatic activity attenuates tumor growth. Mol Cancer Ther. 2005; 4:351–360. DOI: 10.1158/1535-7163.MCT-05-0128 [PubMed: 15767544]
51. Sternlicht MD, Lochter A, Sympson CJ, Huey B, Rougier J-P, Gray JW, Pinkel D, Bissell MJ, Werb Z. The stromal proteinase MMP3/stromelysin-1 promotes mammary carcinogenesis. Cell. 1999; 98:137–146. http://www.ncbi.nlm.nih.gov/pmc/articles/PMC2853255/. [PubMed: 10428026]
52. Radisky DC, Levy DD, Littlepage LE, Liu H, Nelson CM, Fata JE, Leake D, Godden EL, Albertson DG, Nieto MA, Werb Z, Bissell MJ. Rac1b and reactive oxygen species mediate MMP-3-induced EMT and genomic instability. Nature. 2005; 436:123–127. DOI: 10.1038/nature03688 [PubMed: 16001073]
53. Bhowmick NA, Chytil A, Plieth D, Gorska AE, Dumont N, Shappell S, Washington MK, Neilson EG, Moses HL. TGF-β signaling in fibroblasts modulates the oncogenic potential of adjacent

epithelia. Science. 2004; 303:848–851. http://science.sciencemag.org/content/303/5659/848.abstract. [PubMed: 14764882]

54. Straussman R, Morikawa T, Shee K, Barzily-Rokni M, Qian ZR, Du J, Davis A, Mongare MM, Gould J, Frederick DT, Cooper ZA, Chapman PB, Solit DB, Ribas A, Lo RS, Flaherty KT, Ogino S, Wargo JA, Golub TR. Tumour micro-environment elicits innate resistance to RAF inhibitors through HGF secretion. Nature. 2012; 487:500–504. http://dx.doi.org/10.1038/nature11183. [PubMed: 22763439]
55. Mueller MM, Fusenig NE. Friends or foes - bipolar effects of the tumour stroma in cancer. Nat Rev Cancer. 2004; 4:839–849. http://dx.doi.org/10.1038/nrc1477. [PubMed: 15516957]
56. Gore J, Korc M. Pancreatic cancer stroma: friend or foe? Cancer Cell. 2014; 25:711–712. DOI: 10.1016/j.ccr.2014.05.026 [PubMed: 24937454]
57. Chen M, Xiang R, Wen Y, Xu G, Wang C, Luo S, Yin T, Wei X, Shao B, Liu N, Guo F, Li M, Zhang S, Li M, Ren K, Wang Y, Wei Y. A whole-cell tumor vaccine modified to express fibroblast activation protein induces antitumor immunity against both tumor cells and cancer-associated fibroblasts. Sci Rep. 2015; 5:14421.doi: 10.1038/srep14421 [PubMed: 26394925]
58. Lee J, Fassnacht M, Nair S, Boczkowski D, Gilboa E. Tumor immunotherapy targeting fibroblast activation protein, a product expressed in tumor-associated fibroblasts. Cancer Res. 2005; 65:11156–11163. http://cancerres.aacrjournals.org/content/65/23/11156.abstract. [PubMed: 16322266]
59. Loeffler M, Krüger JA, Niethammer AG, Reisfeld RA. Targeting tumor-associated fibroblasts improves cancer chemotherapy by increasing intratumoral drug uptake. J Clin Invest. 2006; 116:1955–1962. DOI: 10.1172/JCI26532 [PubMed: 16794736]
60. Fang J, Xiao L, Joo KI, Liu Y, Zhang C, Liu S, Conti PS, Li Z, Wang P. A potent immunotoxin targeting fibroblast activation protein for treatment of breast cancer in mice. Int J Cancer. 2016; 138:1013–1023. DOI: 10.1002/ijc.29831 [PubMed: 26334777]
61. LeBeau AM, Brennen WN, Aggarwal S, Denmeade SR. Targeting the cancer stroma with a fibroblast activation protein-activated promelittin protoxin. Mol Cancer Ther. 2009; 8:1378–1386. http://mct.aacrjournals.org/content/8/5/1378.abstract. [PubMed: 19417147]
62. Zhen Z, Tang W, Wang M, Zhou S, Wang H, Wu Z, Hao Z, Li Z, Liu L, Xie J. Protein nanocage mediated fibroblast-activation protein targeted photoimmunotherapy to enhance cytotoxic T cell infiltration and tumor control. Nano Lett. 2017; 17:862–869. DOI: 10.1021/acs.nanolett.6b04150 [PubMed: 28027646]
63. Wen XX. Fibroblast activation protein-α-positive fibroblasts promote gastric cancer progression and resistance to immune checkpoint blockade. Oncol Res. 2016; 25:629–640. DOI: 10.3727/096504016X14768383625385 [PubMed: 27983931]
64. Iwasa S, Okada K, Chen W-T, Jin X, Yamane T, Ooi A, Mitsumata M. Increased expression of seprase, a membrane-type serine protease, is associated with lymph node metastasis in human colorectal cancer. Cancer Lett. 2005; 227:229–236. DOI: 10.1016/j.canlet.2004.06.030 [PubMed: 16196122]
65. Chen L, Qiu X, Wang X, He J. FAP positive fibroblasts induce immune checkpoint blockade resistance in colorectal cancer via promoting immunosuppression. Biochem Biophys Res Commun. 2017; 487:8–14. DOI: 10.1016/j.bbrc.2017.03.039 [PubMed: 28302482]
66. Henry LR, Lee H-O, Lee JS, Klein-Szanto A, Watts P, Ross EA, Chen W-T, Cheng JD. Clinical implications of fibroblast activation protein in patients with colon cancer. Clin Cancer Res. 2007; 13:1736–1741. http://clincancerres.aacrjournals.org/content/13/6/1736.abstract. [PubMed: 17363526]
67. Wikberg ML, Edin S, Lundberg IV, Van Guelpen B, Dahlin AM, Rutegård J, Stenling R, Öberg Å, Palmqvist R. High intratumoral expression of fibroblast activation protein (FAP) in colon cancer is associated with poorer patient prognosis. Tumor Biol. 2013; 34:1013–1020. DOI: 10.1007/s13277-012-0638-2
68. Cohen SJ, Alpaugh RK, Palazzo I, Meropol NJ, Rogatko A, Xu Z, Hoffman JP, Weiner LM, Cheng JD. Fibroblast activation protein and its relationship to clinical outcome in pancreatic adenocarcinoma. Pancreas. 2008; 37:154–158. DOI: 10.1097/MPA.0b013e31816618ce [PubMed: 18665076]

69. Kawase T, Yasui Y, Nishina S, Hara Y, Yanatori I, Tomiyama Y, Nakashima Y, Yoshida K, Kishi F, Nakamura M, Hino K. Fibroblast activation protein-α-expressing fibroblasts promote the progression of pancreatic ductal adenocarcinoma. BMC Gastroenterol. 2015; 15:109.doi: 10.1186/s12876-015-0340-0 [PubMed: 26330349]
70. Patsouras D, Papaxoinis K, Kostakis A, Safioleas M, Lazaris A, Nicolopoulou-Stamati P. Fibroblast activation protein and its prognostic significance in correlation with vascular endothelial growth factor in pancreatic adenocarcinoma. Mol Med Rep. 2015; 11:4585–90. DOI: 10.3892/mmr.2015.3259 [PubMed: 25625587]
71. Errarte P, Guarch R, Pulido R, Blanco L, Nunes-Xavier CE, Beitia M, Gil J, Angulo JC, López JI, Larrinaga G. The expression of fibroblast activation protein in clear cell renal cell carcinomas is associated with synchronous lymph node metastases. PLoS One. 2016; 11:e0169105.doi: 10.1371/journal.pone.0169105 [PubMed: 28033421]
72. López JI, Errarte P, Erramuzpe A, Guarch R, Cortés JM, Angulo JC, Pulido R, Irazusta J, Llarena R, Larrinaga G. Fibroblast activation protein predicts prognosis in clear cell renal cell carcinoma. Hum Pathol. 2016; 54:100–105. DOI: 10.1016/j.humpath.2016.03.009 [PubMed: 27063470]
73. Wang H, Wu Q, Liu Z, Luo X, Fan Y, Liu Y, Zhang Y, Hua S, Fu Q, Zhao M, Chen Y, Fang W, Lv X. Downregulation of FAP suppresses cell proliferation and metastasis through PTEN/PI3K/AKT and Ras-ERK signaling in oral squamous cell carcinoma. Cell Death Dis. 2014; 5:e1155.doi: 10.1038/cddis.2014.122 [PubMed: 24722280]
74. Yu H, Yang J, Li Y, Jiao S. The expression of fibroblast activation protein-α in primary breast cancer is associated with poor prognosis. Chinese J Cell Mol Immunol. 2015; 31:370–4. [accessed April 30, 2017] http://www.ncbi.nlm.nih.gov/pubmed/25744843.
75. Jia J, Martin T, Ye L, Jiang W. FAP-α (Fibroblast activation protein-α) is involved in the control of human breast cancer cell line growth and motility via the FAK pathway. BMC Cell Biol. 2014; 15:16.doi: 10.1186/1471-2121-15-16 [PubMed: 24885257]
76. Yuan D, Liu B, Liu K, Zhu G, Dai Z, Xie Y. Overexpression of fibroblast activation protein and its clinical implications in patients with osteosarcoma. J Surg Oncol. 2013; 108:157–162. DOI: 10.1002/jso.23368 [PubMed: 23813624]
77. Liao Y, Ni Y, He R, Liu W, Du J. Clinical implications of fibroblast activation protein-α in non-small cell lung cancer after curative resection: a new predictor for prognosis. J Cancer Res Clin Oncol. 2013; 139:1523–1528. DOI: 10.1007/s00432-013-1471-8 [PubMed: 23835897]
78. Saigusa S, Toiyama Y, Tanaka K, Yokoe T, Okugawa Y, Fujikawa H, Matsusita K, Kawamura M, Inoue Y, Miki C, Kusunoki M. Cancer-associated fibroblasts correlate with poor prognosis in rectal cancer after chemoradiotherapy. Int J Oncol. 2011; 38:655–63. DOI: 10.3892/ijo.2011.906 [PubMed: 21240461]
79. Ju MJ, Qiu SJ, Fan J, Xiao YS, Gao Q, Zhou J, Li YW, Tang ZY. Peritumoral activated hepatic stellate cells predict poor clinical outcome in hepatocellular carcinoma after curative resection. Am J Clin Pathol. 2009; 131:498–510. DOI: 10.1309/AJCP86PPBNGOHNNL [PubMed: 19289585]
80. De Wever O, Demetter P, Mareel M, Bracke M. Stromal myofibroblasts are drivers of invasive cancer growth. Int J Cancer. 2008; 123:2229–2238. DOI: 10.1002/ijc.23925 [PubMed: 18777559]
81. Vong S, Kalluri R. The role of stromal myofibroblast and extracellular matrix in tumor angiogenesis. Genes Cancer. 2011; 2:1139–1145. DOI: 10.1177/1947601911423940 [PubMed: 22866205]
82. Hecht JR, Bendell JC, Vyushkov D, Bencardino K, Verma UN, Yang Y, Thai DL. A phase II, randomized, double-blinded, placebo-controlled study of simtuzumab or placebo in combination with FOLFIRI for the second line treatment of metastatic KRAS mutant colorectal adenocarcinoma. J Clin Oncol. 2015; 33:243–e23. DOI: 10.1200/jco.2015.33.15_suppl.3537
83. Benson A III, Bendell J, Wainberg ZA, Vyushkov D, Acs P, Kudrik F, Dong H, Thai D. 618PD A phase 2 randomized, double-blind, placebo controlled study of simtuzumab or placebo in combination with gemcitavine for the first line treatment of pancreatic adenocarcinoma. Ann Oncol. 2014; 25:iv211–iv211. http://dx.doi.org/10.1093/annonc/mdu334.4.
84. Raghu G, Brown KK, Collard HR, Cottin V, Gibson KF, Kaner RJ, Lederer DJ, Martinez FJ, Noble PW, Song JW, Wells AU, Whelan TPM, Wuyts W, Moreau E, Patterson SD, Smith V, Bayly S, Chien JW, Gong Q, Zhang JJ, O'Riordan TG. Efficacy of simtuzumab versus placebo in patients

with idiopathic pulmonary fibrosis: a randomised, double-blind, controlled, phase 2 trial. Lancet Respir Med. 2017; 5:22–32. DOI: 10.1016/S2213-2600(16)30421-0 [PubMed: 27939076]

85. Meyer KC. Great expectations for simtuzumab in IPF fall short. Lancet Respir Med. 2017; 5:2–3. DOI: 10.1016/S2213-2600(16)30420-9 [PubMed: 27939077]
86. Rhim AD, Oberstein PE, Thomas DH, Mirek ET, Palermo CF, Sastra SA, Dekleva EN, Saunders T, Becerra CP, Tattersall IW, Westphalen CB, Kitajewski J, Fernandez-Barrena MG, Fernandez-Zapico ME, Iacobuzzio-Donahue C, Olive KP, Stanger BZ. Stromal elements act to restrain, rather than support, pancreatic ductal adenocarcinoma. Cancer Cell. 2014; 25:735–747. DOI: 10.1016/j.ccr.2014.04.021 [PubMed: 24856585]
87. Olive KP, Jacobetz MA, Davidson CJ, Gopinathan A, McIntyre D, Honess D, Madhu B, Goldgraben MA, Caldwell ME, Allard D, Frese KK, DeNicola G, Feig C, Combs C, Winter SP, Ireland H, Reichelt S, Howat WJ, Chang A, Dhara M, Wang L, Rückert F, Grützmann R, Pilarsky C, Izeradjene K, Hingorani SR, Huang P, Davies SE, Plunkett W, Egorin M, Hruban RH, Whitebread N, McGovern K, Adams J, Iacobuzio-Donahue C, Griffiths J, Tuveson DA. Inhibition of hedgehog signaling enhances delivery of chemotherapy in a mouse model of pancreatic cancer. Science. 2009; 324:1457–1461. DOI: 10.1126/science.1171362 [PubMed: 19460966]
88. Lee JJ, Perera RM, Wang H, Wu DC, Liu XS, Han S, Fitamant J, Jones PD, Ghanta KS, Kawano S, Nagle JM, Deshpande V, Boucher Y, Kato T, Chen JK, Willmann JK, Bardeesy N, Beachy PA. Stromal response to Hedgehog signaling restrains pancreatic cancer progression. Proc Natl Acad Sci. 2014; 111:E3091–E3100. DOI: 10.1073/pnas.1411679111 [PubMed: 25024225]
89. Sherman MH, Yu RT, Engle DD, Ding N, Atkins AR, Tiriac H, Collisson EA, Connor F, Van Dyke T, Kozlov S, Martin P, Tseng TW, Dawson DW, Donahue TR, Masamune A, Shimosegawa T, Apte MV, Wilson JS, Ng B, Lau SL, Gunton JE, Wahl GM, Hunter T, Drebin JA, O'Dwyer PJ, Liddle C, Tuveson DA, Downes M, Evans RM. Vitamin D receptor-mediated stromal reprogramming suppresses pancreatitis and enhances pancreatic cancer therapy. Cell. 2014; 159:80–93. DOI: 10.1016/j.cell.2014.08.007 [PubMed: 25259922]
90. Beacham, DA., Amatangelo, MD., Cukierman, E. Curr Protoc Cell Biol. John Wiley & Sons, Inc; 2001. Preparation of Extracellular Matrices Produced by Cultured and Primary Fibroblasts.
91. Brisson BK, Mauldin EA, Lei W, Vogel LK, Power AM, Lo A, Dopkin D, Khanna C, Wells RG, Puré E, Volk SW. Type III collagen directs stromal organization and limits metastasis in a murine model of breast cancer. Am J Pathol. 2015; 185:1471–1486. DOI: 10.1016/j.ajpath.2015.01.029 [PubMed: 25795282]
92. Blissett AR, Garbellini D, Calomeni EP, Mihai C, Elton TS, Agarwal G. Regulation of collagen fibrillogenesis by cell-surface expression of kinase dead DDR2. J Mol Biol. 2009; 385:902–911. DOI: 10.1016/j.jmb.2008.10.060 [PubMed: 18996394]

Highlights

- Fibroblast activation protein (FAP) and alpha-smooth muscle actin (αSMA) identify distinct, yet overlapping, activated fibroblast subsets in a variety of pathophysiological settings, including wound healing, fibrosis, and tumorigenesis.
- A convergence of extracellular (ECM) composition, elasticity, and transforming growth factor beta (TGF-β) signaling governs activated fibroblast phenotypic heterogeneity.
- Low stiffness, fibronectin-rich ECMs promote the $FAP^{Hi}\alpha SMA^{Low}$ reactive fibroblast phenotype.
- Stiff and/or collagen I-rich ECMs promote the $FAP^{Low}\alpha SMA^{Hi}$ myofibroblast phenotype.
- Gene expression profiling indicates unique functionality of FAP^{Hi} and αSMA^{Hi} activated fibroblast subsets in tissue remodeling.

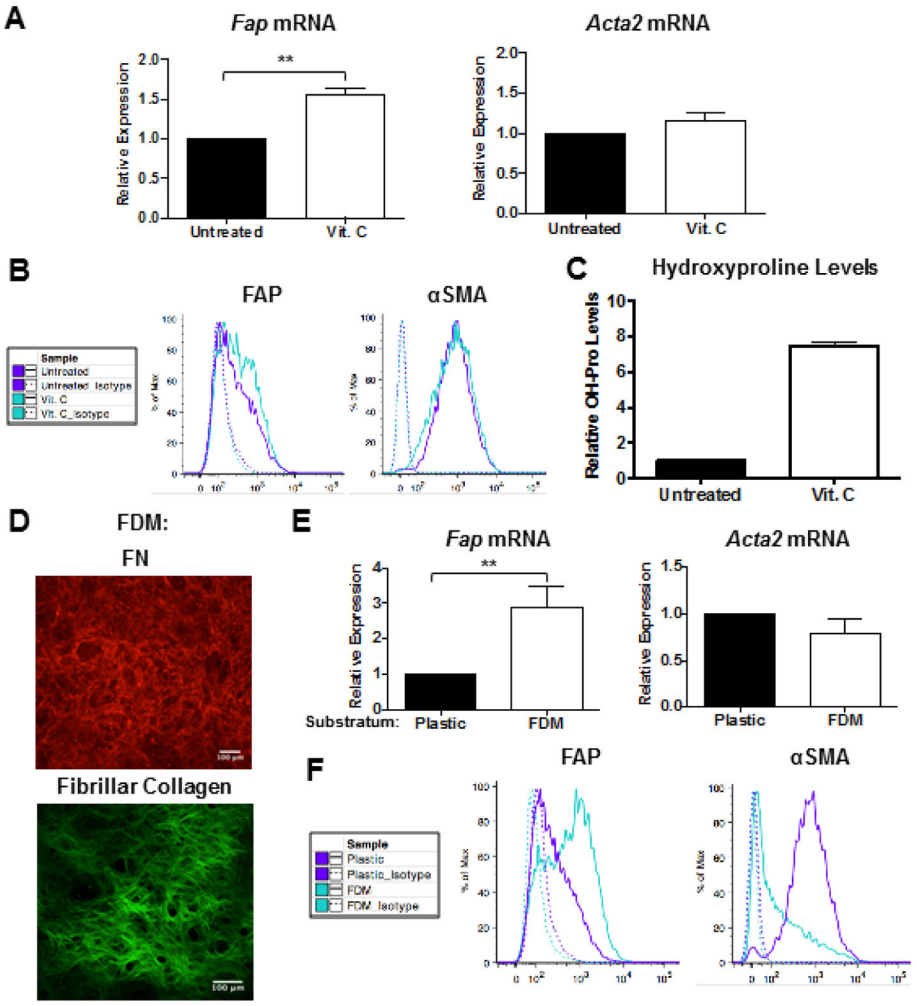

Figure 1. Substratum directs activated fibroblast phenotypic heterogeneity

QRT-PCR (A) and representative flow cytometric analysis (B) of FAP and αSMA expression in fibroblasts cultured in 10% serum on tissue culture-treated plastic in the presence or absence of 75 μg/ml ascorbic acid (Vit. C) for 4 days. Data were compiled from 4 independent experiments and bar graphs depict the mean +/− SEM. (C) Collagen levels (as measured via hydroxyproline content) in FDMs deposited by fibroblasts in the presence or absence of 75 μg/ml Vit. C. Data were compiled from 2 independent experiments and bar graphs depict the mean +/− SEM. (D) Representative IF staining of FN and two-photon second harmonic generation imaging of fibrillar collagen in lung FDMs. QRT-PCR (E) and representative flow cytometric analysis (F) of FAP and αSMA expression in fibroblasts in 10% serum on tissue culture-treated plastic or FDM for 4 days. Data were compiled from 4 independent experiments and bar graphs depict the mean +/− SEM.

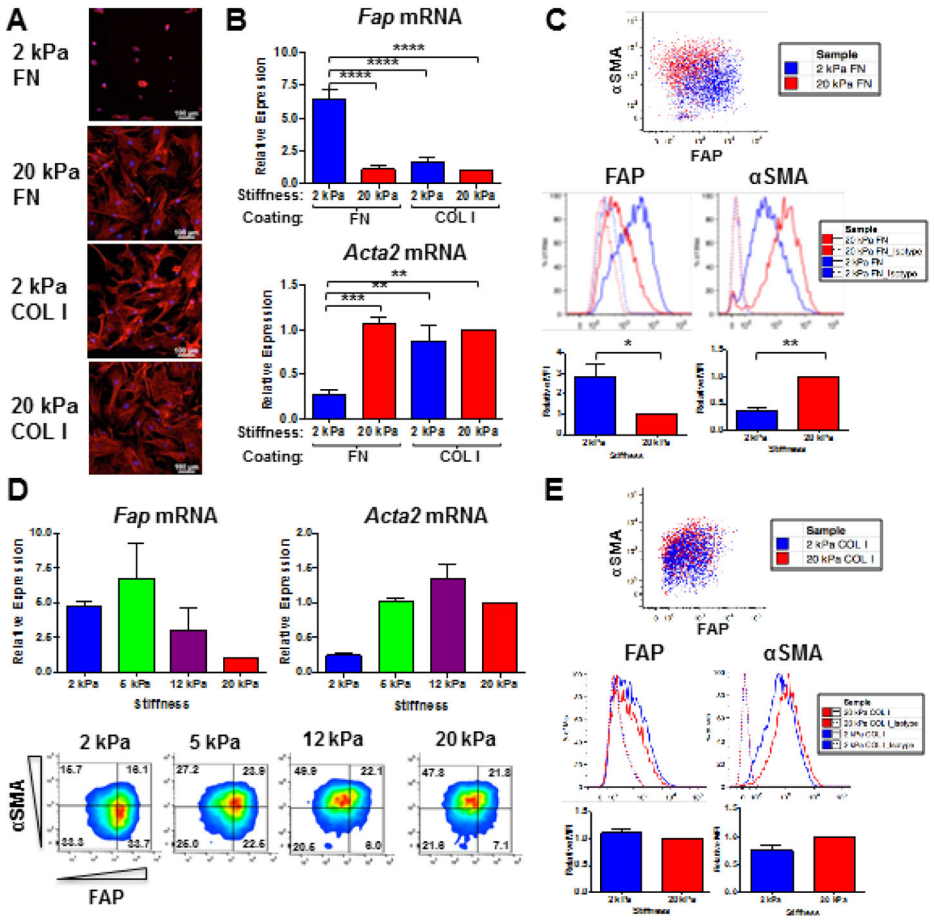

Figure 2. ECM composition and elasticity govern activated fibroblast phenotypic heterogeneity

Representative phalloidin staining of the actin cytoskeleton (A) and *Fap* and *Acta2* gene expression (B) in fibroblasts cultured in 10% serum on 2 versus 20 kPa FN- or COL I-coated hydrogels for 72 hours. Data were compiled from 4 independent experiments and bar graphs depict the mean +/− SEM. (C) Representative flow cytometric analysis, including quantification of relative median fluorescent intensities (MFI) for FAP and αSMA expression in fibroblasts cultured in 10% serum on 2 kPa (blue) versus 20 kPa (red) FN-coated hydrogels for 72 hours. Data were compiled from 3 independent experiments and bar graphs depict the mean +/− SEM. (D) QRT-PCR (top) and flow cytometric analysis (bottom) of FAP and αSMA expression in fibroblasts cultured in 10% serum on 2, 5, 12, and 20 kPa FN-coated hydrogels for 72 hours. Data were compiled from 2 independent experiments and bar graphs depict the mean +/− SEM. (E) Representative flow cytometric analysis, including quantification of relative MFI for FAP and αSMA expression in lung fibroblasts cultured in 10% serum on 2 kPa (blue) versus 20 kPa (red) COL I-coated hydrogels for 72 hours. Data were compiled from 3 independent experiments and bar graphs depict the mean +/− SEM.

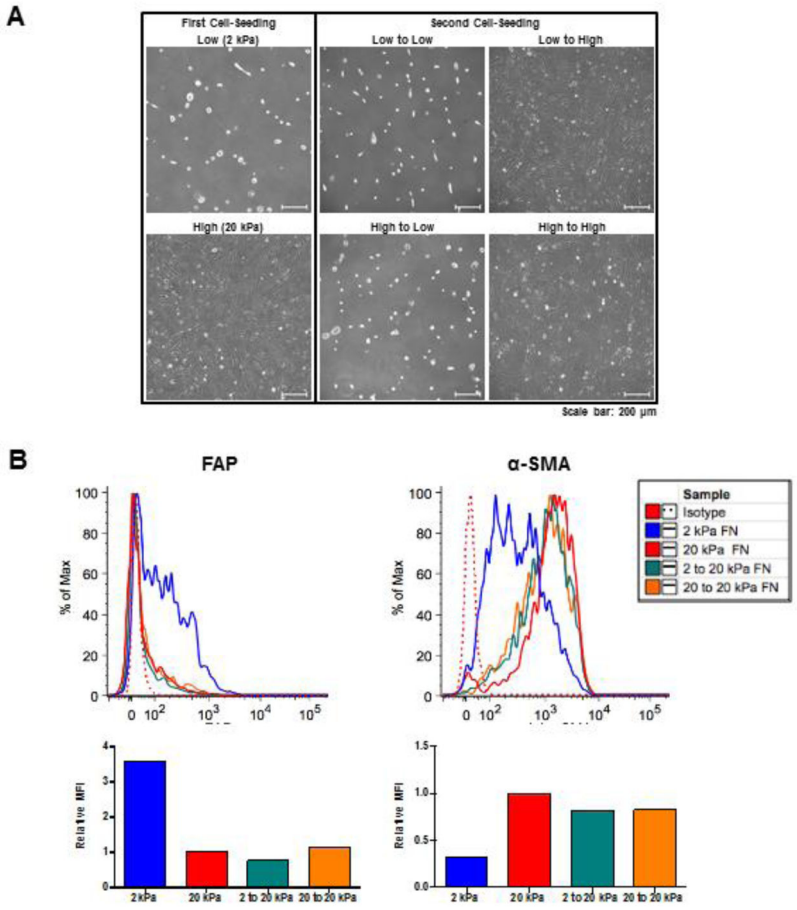

Figure 3. FAP^{Hi} and αSMA^{Hi} fibroblasts exhibit morphologic and phenotypic plasticity

Fibroblasts were serially cultured (in 10% FCS DMEM) first on either 2 or 20 kPa FN-coated hydrogels for 72 hours, and then cells recovered by trypsinization from each of these groups were cultured for a second time on either 2 or 20 kPa FN-coated hydrogels for an additional 72 hours. At both rounds 1 and 2, cell monolayers were analyzed by phase contrast microscopy and cell suspensions were analyzed by flow cytometry. Representative phase contrast images (A) and flow cytometric analysis (B), including quantification of relative MFI for FAP and αSMA expression, are shown.

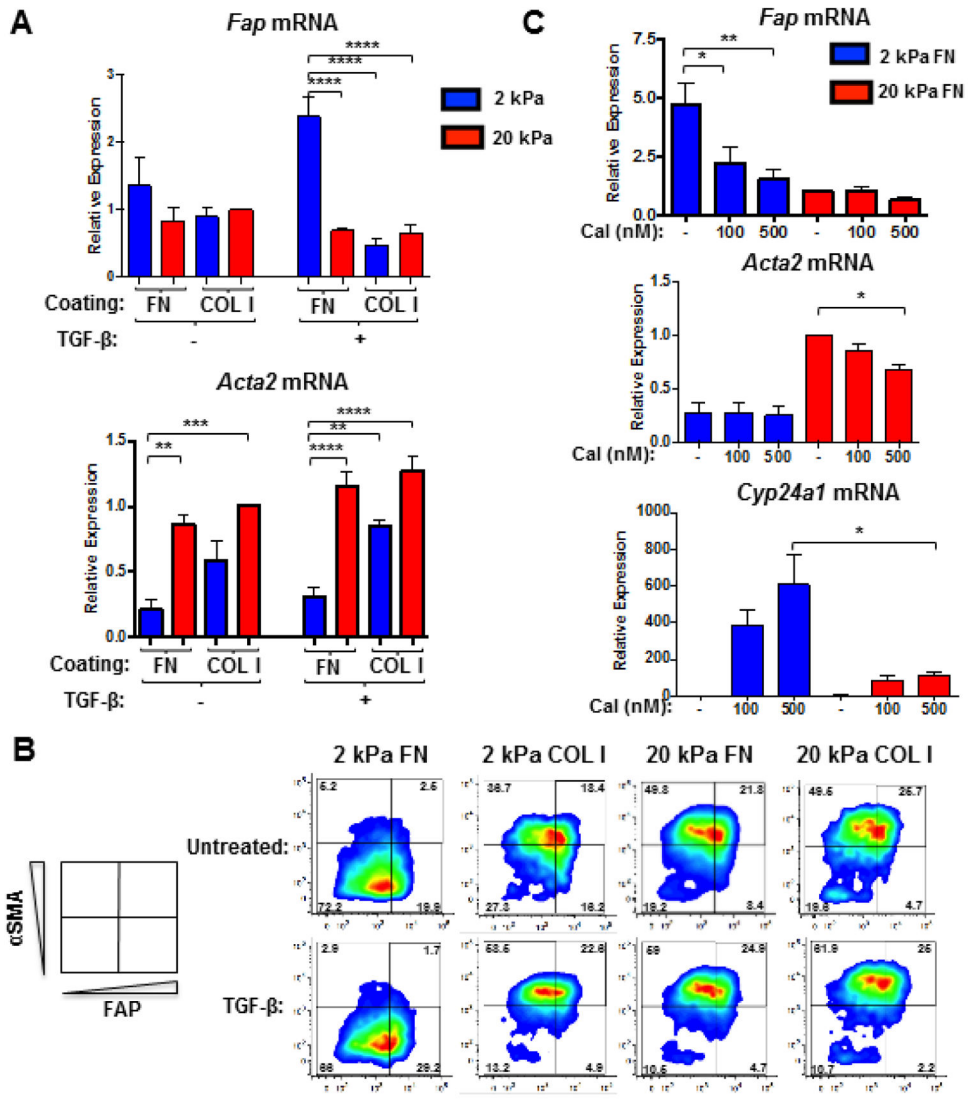

Figure 4. Fibroblast differentiation in response to TGF-β is governed by ECM composition and elasticity

QRT-PCR (A) and flow cytometric analysis (B) of FAP and αSMA expression in fibroblasts that were seeded in 1% serum on 2 versus 20 kPa COL I- or FN-coated hydrogels, allowed to adhere overnight, and subsequently treated with 2 ng/ml TGF-β for 48 (A) or 72 hours (B). Data were compiled from 4 independent experiments and bar graphs depict the mean +/− SEM. (C) QRT-PCR analysis of *Fap*, *Acta2*, and *Cyp24a1* gene expression in fibroblasts that were seeded in 10% serum on FN-coated hydrogels (2 or 20 kPa), allowed to adhere overnight, and subsequently treated with calcipotriol (Cal; 100 or 500 nM) or vehicle control for 48 hours. Data were compiled from 3 independent experiments and bar graphs depict the mean +/− SEM.

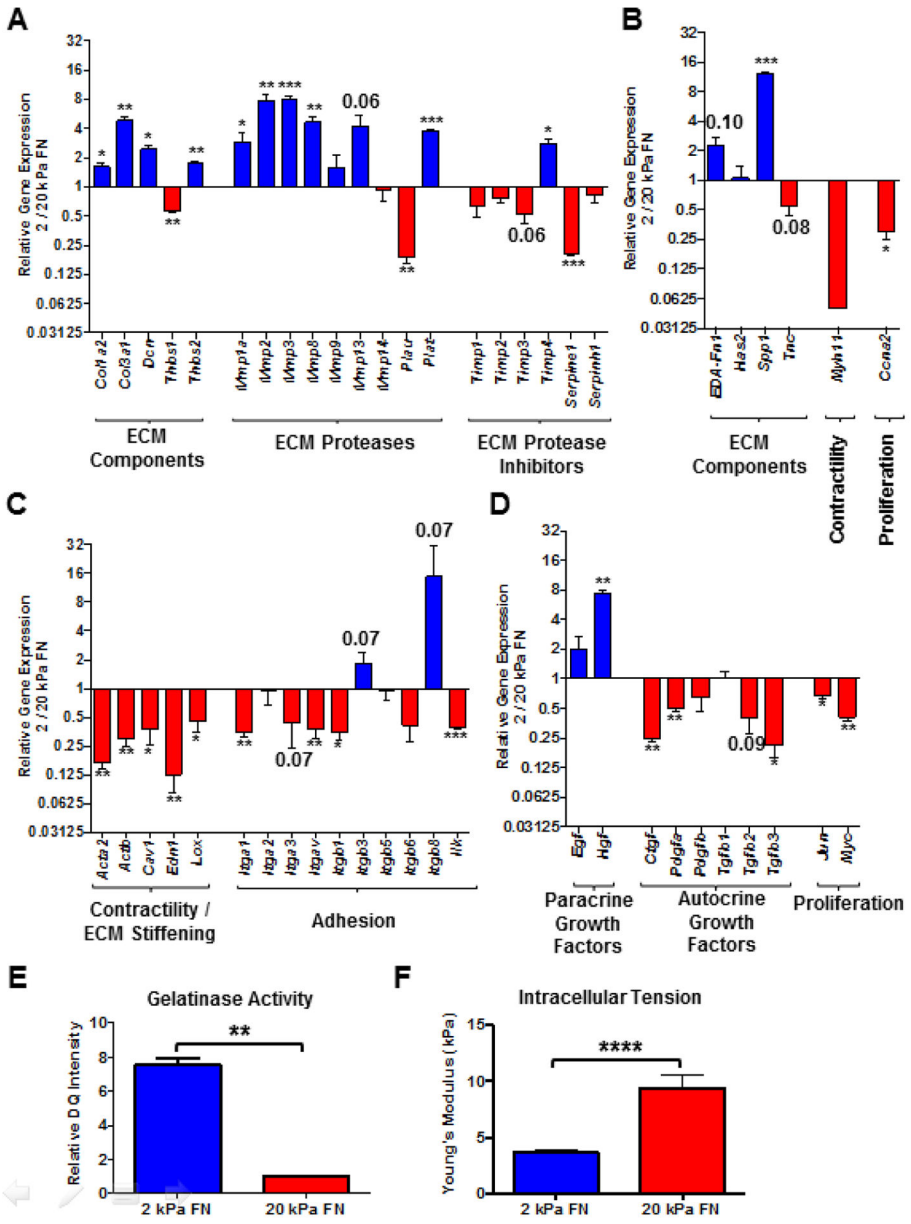

Figure 5. Gene expression profiling and functional tests indicate that FAP^{Hi} reactive fibroblasts predominantly synthesize and proteolyze ECM, while αSMA^{Hi} myofibroblasts mediate contraction

Comparison of gene expression profiles, assessed via Qiagen Fibrosis Gene Expression Array (A, C, and D) and independent qRT-PCR analyses (B), of fibroblasts cultured in 10% serum on 2 (FAP^{Hi} fibroblasts) or 20 kPa (αSMA^{Hi} fibroblasts) FN-coated hydrogels for 72 hours. Relative gene expression (FAP^{Hi}/αSMA^{Hi} fibroblasts) of ECM proteases (A), ECM protease inhibitors (A), ECM and matricellular components (A and B), contractile mediators (B and C), integrin subunits (C), growth factors (D), and proliferative mediators (B and D). Data were compiled from 3 independent experiments and bar graphs depict the mean +/− SEM. (E) Quantification of relative DQ intensity of fibroblasts that were cultured on 2 or 20 kPa FN-coated hydrogels for 48 hours, and then incubated with DQ gelatin for an additional

24 hours. Data were compiled from 3 independent experiments and bar graphs depict the mean +/− SEM. (F) Atomic force microscopy (AFM) measurements of intracellular tension in fibroblasts cultured in 10% serum on 2 or 20 kPa FN-coated hydrogels for 72 hours. Bar graph depicts the mean +/− SEM (n=10 cells).

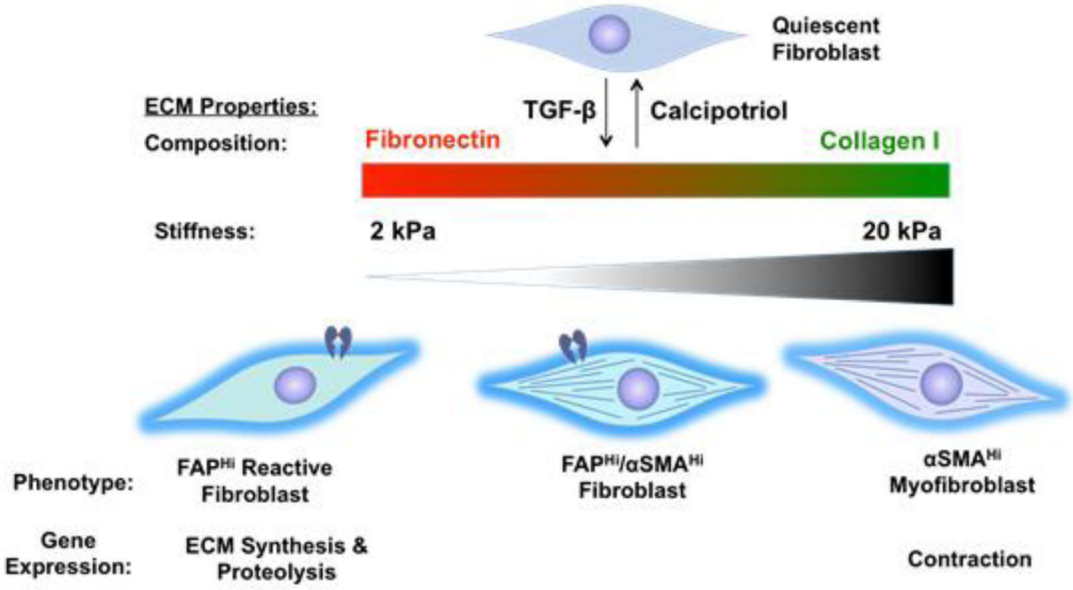

Figure 6. A convergence of ECM composition, elasticity, and TGF-β signaling governs activated fibroblast phenotypic heterogeneity

In FN-rich ECMs of low stiffness, TGF-β promotes the $FAP^{Hi}\alpha SMA^{Low}$ reactive fibroblast phenotype. Conversely, TGF-β promotes the $FAP^{Low}\alpha SMA^{Hi}$ myofibroblast phenotype in the context of stiff and/or COL I-rich ECMs. Gene expression profiling indicates unique functionality of these divergent fibroblast subsets in tissue remodeling, with FAP^{Hi} reactive fibroblasts exhibiting an ECM synthetic and proteolytic phenotype, and αSMA^{Hi} myofibroblasts exhibiting a contractile and proliferative phenotype.